

Structural Parameters in Relation to the Rheological Behavior and Properties of PP/EPR In-Reactor Alloy Synthesized by Multi-Stage Sequential Polymerization

H. Bagheri,¹ M. Nekoomanesh,¹ S. Hakim,¹ Y. Jahani,¹ Z. Q. Fan²

¹Iran Polymer and Petrochemical Institute, Tehran, Iran

²Department of Polymer Science and Engineering, Zhejiang University, Hangzhou, 310027, People's Republic of China

Received 27 June 2010; accepted 11 December 2010

DOI 10.1002/app.33951

Published online 11 April 2011 in Wiley Online Library (wileyonlinelibrary.com).

ABSTRACT: The morphology and molecular structure of an in-reactor polypropylene/ethylene propylene rubber alloy, synthesized by multi-stage sequential polymerization, were studied with respect to the rheological behavior and final properties of the alloy. The polymer alloys, based on different structural morphologies, were characterized by SEM, GPC, ¹³C NMR, DSC, rheological analysis, and mechanical testing. The scanning electron microscopy of samples showed that the size of the dispersed phase particles is decreased as the switch frequency of copolymerization timing is increased. The GPC results showed that switch frequency slightly altered the molecular weight distribution of the copolymer although it had no effect on PP homopolymer. ¹³C NMR results were used for the evaluation of compatibility between the

two phases with changes in switch frequency. DSC results showed that T_m and T_c were almost independent of switch frequency, even though the size of dispersed phase was decreased and the blend crystal content increased with ΔH of about 13%. The small amplitude oscillation rheometry showed that storage modulus and viscosity shifted to higher values when switch frequency increased. In studying the mechanical properties it was revealed that, especially the impact strength increased by about 62% when the size of the dispersed particles was decreased. © 2011 Wiley Periodicals, Inc. *J Appl Polym Sci* 121: 3332–3339, 2011

Key words: in-reactor alloy; polymerization; structure-properties relationship; PP/EPR blend

INTRODUCTION

Polypropylene (PP) is a very versatile thermoplastic material with a wide range of applications in the plastics industry.¹ For engineering applications, polypropylene shows limited toughness, especially at room and low temperatures. Blending of immiscible polymers is a very useful technical process to obtain materials with improved properties.²

The versatility of an *in situ* copolymerization of an alloy in a process known as “in-reactor alloy” facilitates the production of an immiscible alloy in one single reactor. In this way, alloys with high ethylene-propylene rubber content are produced in two steps. In the first step, propylene is polymerized into a polypropylene homopolymer by a stereospecific catalyst system. In the second step, a mixture of ethylene and propylene are copolymerized using the same catalyst.³ Zhang et al.⁴ studied the influence of copolymerization conditions on the structure and

properties of PP/EPR *in situ* blends. They showed that the properties of the blends are highly dependent on the amount of copolymer fractions, their distribution, and resulting chain structures and notably, the impact strength is influenced by both the random and block copolymer portions in a complex manner. Also, they found that the synergistic effect between the random and segmented copolymers is a key factor for showing high impact strength at low temperatures.⁵ Lin et al.⁶ investigated the ethylene component in the PP CATALLOY (a polypropylene polymer production process in gaseous phase) and showed that while it acts as a nucleating agent and induces higher crystallization rate, it reduces the crystallinity and spherulite size. Xu et al.⁷ showed that alloys with smaller crystalline particles enhance compatibility between the matrix and dispersed phases. Chen et al.⁸ showed that the dispersed phase in high-impact polypropylene (HIPP) exhibits a multilayered core-shell structure including the inner core, intermediate layer, and outer shell, which were mainly composed of PE (including PE long blocks), EPR and PE-PP multi-block copolymers, respectively. The outer shell is a compatibilizing layer bridging the intermediate layers (EPR phase) and

Correspondence to: M. Nekoomanesh (m.nekoomanesh@ippi.ac.ir).

the PP matrix. Also the finding of Jiang et al.⁹ showed that block copolymer fractions function as compatibilizers, which are localized at the interface between the matrix and the EPR dispersed phase. Xu et al.¹⁰ found that the large particles are rich in propylene homopolymer and ethylene-propylene block copolymer, whereas the small particles contain more ethylene-propylene random copolymer and copolymer with a transient microstructure. Mei et al.¹¹ from Basell Company reported a new PP manufacturing platform based on the innovative multi-stage circulating reactor (MZCR), with a unique way to produce polymers. This would allow the production of polymeric materials with superior physical properties and processability. Dong et al.¹² succeeded to simulate this technique in their lab. They proposed a new method to improve the particle size of dispersed phase in (PP) reactor alloys without any change in the catalyst system. In this method, a multi-stage sequential polymerization process was used to improve the morphology and mechanical properties of PP/EPR in-reactor alloys. It is also reported that at higher switch frequency in copolymerization stage, the molecular chain architecture of the alloys is not detectable, and the size of EPR particles decreases with a uniform size distribution and the alloy shows a much more improved toughness-stiffness balance compared to PP/EPR alloy which is produced by a conventional two-step process.

In the previous work, we reported the rheological characterization of PP/EPR in-reactor alloys synthesized by a multi-stage sequential polymerization process, while a relationship between the rheological and morphological characteristics was obtained, with the specific role of temperature in relation to rheological properties.¹³

In continuation, the present work involves the preparation of PP/EPR in-reactor alloys via multi-stage sequential gas-phase homopolymerization of propylene and gas-phase ethylene-propylene copolymerization in circular mode.

We also demonstrate the effect of structural parameters on the final properties of these copolymer compounds by morphological studies (SEM), molecular weight distribution (GPC), interfacial adhesion (NMR), thermal analysis (DSC), and rheological characteristics.

EXPERIMENTAL

Synthesis of PP/EPR in-reactor alloy

The PP/EPR in-reactor alloy samples were synthesized through a multi-stage sequential polymerization process. In the first prepolymerization stage, the slurry polymerization of propylene was carried out

TABLE I
The Polymerization Time and Switching Sequence of PP/EPR In-Reactor Alloys

| Code | Homopolymerization time (min) | Copolymerization time (min) | Switching frequency |
|------|-------------------------------|-----------------------------|---------------------|
| EP20 | 60 | 20 | 1 |
| EP10 | 30 | 10 | 2 |
| EP5 | 15 | 5 | 4 |

at 0.1 MPa and 50°C for 30 min in *n*-heptane as solvent. Then, propylene was added to the reactor at 0.6 MPa to start its homopolymerization. Propylene was homopolymerized within 60 min at 60°C. Then, the solvent and propylene were evacuated at 5 mmHg for 3 min and the circular process of the gas-phase mode was started. The mixture of ethylene and propylene monomers, at a fixed ratio, was fed into the reactor at a constant pressure of 0.4 MPa and 60°C temperature. After copolymerization of ethylene and propylene for a predetermined time, the ethylene-propylene mixture was removed by evacuation at 5 mmHg for 3 min, and then propylene was constantly fed into the reactor at 0.6 MPa pressure and 60°C temperature. The sequences of propylene homopolymerization were followed by ethylene-propylene copolymerization and subsequently the propylene homopolymerization was performed under the same conditions as stated above for a number of times preset switching process. Finally, the circular reaction mode was carried out for 80 min.

In this way, the sample EP20 was synthesized by ethylene-propylene copolymerization for 20 min and then propylene homopolymerization was carried out for 60 min. In other words, the switching number of this sample was designated as 1. The sample EP10, as switching number 2, was synthesized by ethylene-propylene copolymerization for 10 min followed by propylene homopolymerization for 30 min. Overall, the total copolymerization time was 80 min. Similarly, the switching number 4 for EP5 proceeded as above. The above information is summarized in Table I. In any case, although the total copolymerization time for all samples was equal but the timing allocation for each stage was different.

Scanning electron microscopy

The morphology and dispersion state of EPR phase in the PP matrix were investigated using a JSM-T20 scanning electron microscope. The samples, compression molded at 14.5 MPa and 180°C for 5 min, were fractured in liquid nitrogen. The fractured surfaces were dipped into xylene and etched ultrasonically for 5 min at room temperature. The fractured surface of the samples after etching was gold coated before SEM study.

Fractionation of alloy

To achieve a uniform separation of EPR, the samples were extracted in boiling *n*-heptane in a Kumagawa extractor for 12 h. The extract solution was concentrated and precipitated by ethanol and the extracted substance was washed and subsequently dried in vacuum.

Measurement of molecular weight

Molecular weights of the samples were determined by a PL-220 gel permeation chromatography (GPC) at 150°C using trichlorobenzene as a solvent at the concentration of 0.2–0.3 w/v% and 1.0 mL min⁻¹ flow rate.

¹³C NMR analysis

¹³C NMR spectra of the fractions were obtained on a Varian Mercury Plus 300 NMR spectrometer at 75 MHz. The concentration of the polymer solution was 10 wt % prepared in *o*-dichlorobenzene-*d*₄ as a solvent. The spectra were recorded at 120°C. Chromium triacetylacetonate (2–3 mg) was added to each sample to shorten the relaxation time and ensure exact quantitative results. Broadband decoupling with a pulse delay of 3 s was employed and finally, 5000 transients were collected.

Thermal analysis

The DSC measurements were carried out on a Perkin–Elmer Pyris-1 calorimeter. About 5 mg of the polymer sample was sealed in an aluminum pan. The polymer sample was first heated to 220°C at a rate of 5°C min⁻¹ under nitrogen atmosphere and held for 3 min to remove its thermal history. Then it was cooled to 40°C at a rate of 5°C min⁻¹, held for 5 min, and subsequently heated to 250°C at a rate of 5°C min⁻¹. Both of the cooling and heating traces were recorded.

Oscillation rheometry

Rheological properties of the samples were evaluated by a Rheometric Scientific ARES Rheometer [902-30004]. Circular samples of each 25-mm diameter and 1.4-mm thickness were prepared by compression molding process. The responses of the melts in the linear viscoelastic range of oscillatory deformation were evaluated at 180°C under nitrogen atmosphere in the angular frequency range of 0.01 to 100 rad s⁻¹ with 1-mm gap.

Measurement of mechanical properties

The notched charpy impact strength of the compression molded samples was measured on a Ceast

impact strength tester according to ASTM D256. Flexural modulus of the samples was measured according to ASTM D790 on a Shimadzu AG-500A electronic tester. Five parallel measurements were made and the average values were recorded.

RESULTS AND DISCUSSION

Morphology of copolymers

Three HIPP samples were produced with three different switch frequencies. For all samples, the polymerization parameters such as: total homopolymerization time, temperature profile, pressure, and all other parameters were the same, except copolymerization time which was divided into several zones for each sample, where the switch frequency altered by 5, 10, and 20 min. Therefore, time distribution of copolymerization changed the morphology and size of the dispersed phase, and by this we intended to break the dispersed phases into smaller sizes.

Figure 1 shows SEM micrographs of the fractured surfaces of three PP/EPR in-reactor alloys that were prepared by etching with xylene. As shown in Figure 1 for EP20, there are many large cavities in non-uniform distribution. However, the average cavity size of EP10 is smaller than that of EP20 and with more uniformity. EP5 has the smallest cavity size with the most uniform distribution as compared with the other two samples (EP10 and EP20). According to Figure 1, with the increased switch frequency the size of the EPR dispersed phase is predictably decreased which is in accordance with our previous work.¹³ The increase in switch frequency distributes copolymerization time to create more uniform dispersed phase as reported by Dong et al.¹²

Gel permeation chromatography

Figure 2(a) shows GPC results for *n*-heptane insoluble fractions of EP5 and EP20. It can be seen that molecular weight distribution is almost similar in both samples, and even a slight shift to high molecular weight could be considered as an experimental error, for the reason that the polymerization conditions such as catalyst, total time and monomer pressure are exactly the same for all samples.

GPC results for the *n*-heptane soluble fractions of EP5 and EP20 can be seen in Figure 2(b). A soluble fraction is a mixture of random, block copolymer and low molecular weight polymers. This figure shows that the molecular weight distribution of EP20 is slightly narrower than that of EP5. However, the differences are not very significant again due to the similar polymerization conditions.

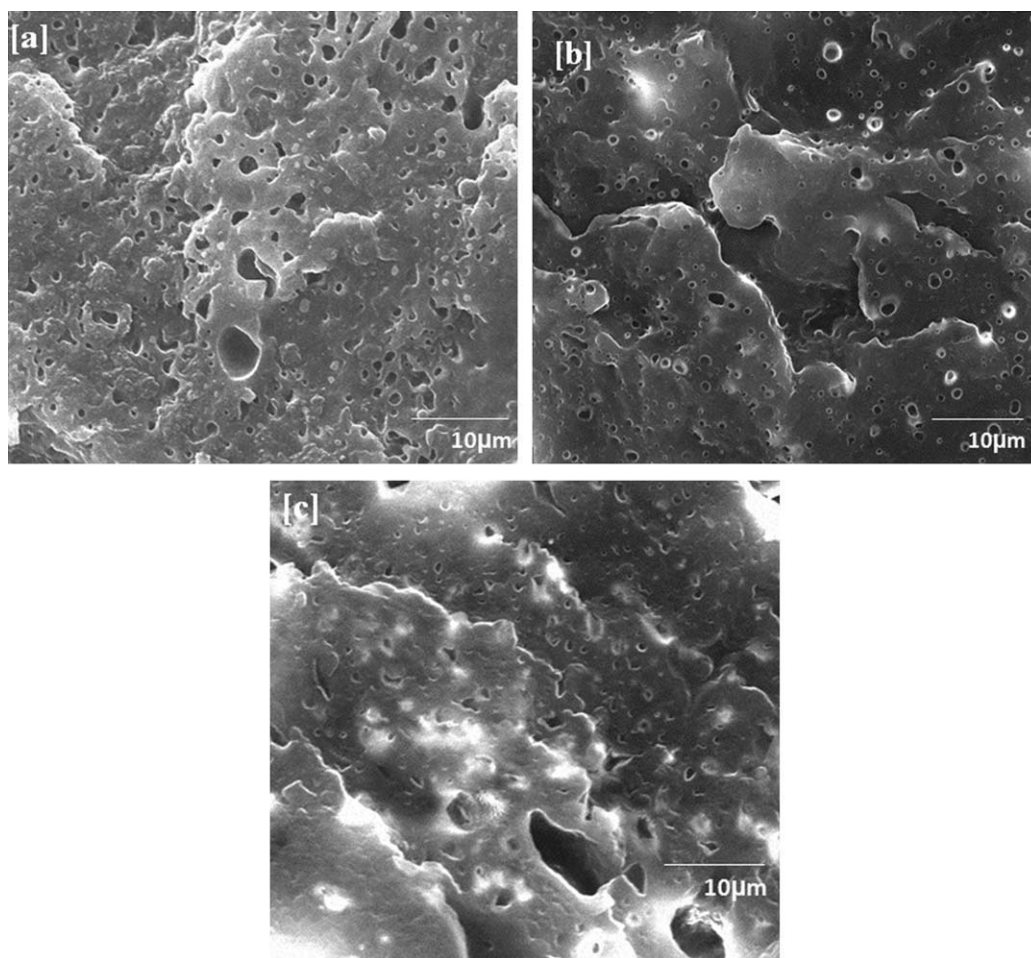


Figure 1 SEM photographs of the impact fracture surface of; (a) EP20, (b) EP10, (c) EP5.

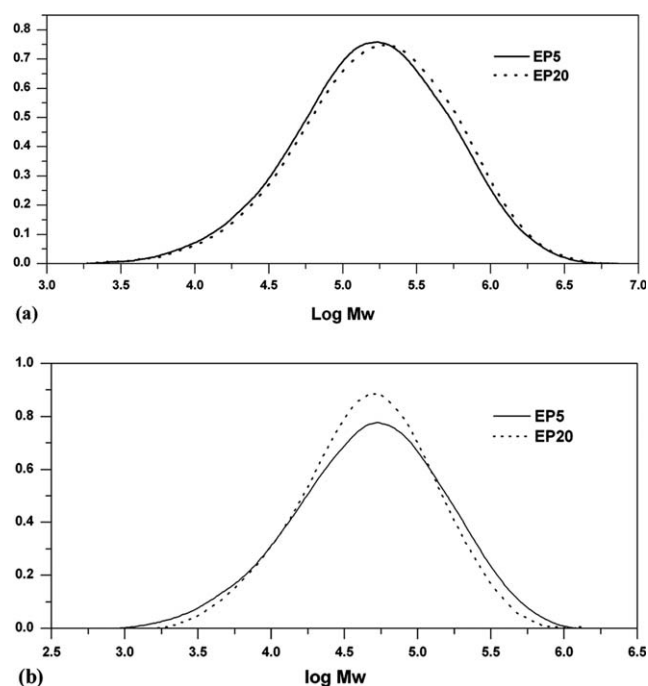


Figure 2 GPC curves for (a) insoluble fraction, (b) soluble fraction.

It can be concluded that switch frequency has a slight effect on the molecular weight distribution of copolymer, though no effect on the homopolymer. These results match with Dong et al.'s findings.¹² They showed in their experimental data that under the same polymerization conditions, all samples have identical structures and the switch frequency has no effect on the structure of the blends either.

¹³C NMR analysis

Two different samples were collected from Kumagawa analysis: PP-rich sample as insoluble fraction and EPR sample as soluble fraction. To investigate the efficiency of separation, ¹³C NMR was used for the insoluble fraction and only three chemical shifts were observed for PP samples at 21.61, 24.49, and 46.11 ppm in accordance with the findings reported by Randall and Hsieh.¹⁴ Figure 3(a) indicates that there are some chemical shifts at 29.77, belonging to the EPR *b*-copolymer but no such chemical shift is observed in Figure 3(b) belonging to EP20. This

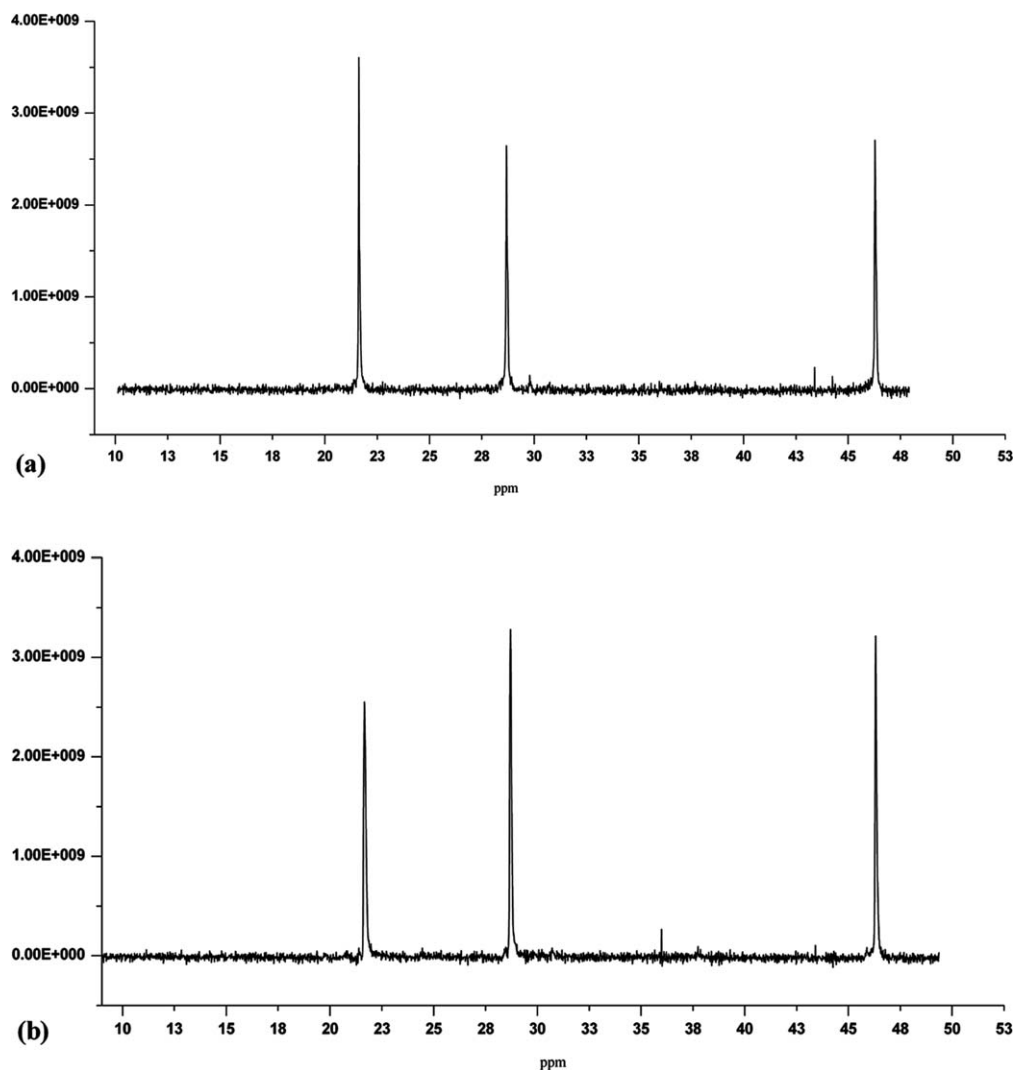


Figure 3 ^{13}C NMR spectra of insoluble fraction (a) EP5, (b) EP20.

means that there is no EPR residual present in the extracted EP20.

On the other hand, chemical shifts observed at 21.66 for both samples show that this peak is higher for EP5 than for EP20. This is an indication of the presence of high PP rich *b*-copolymer in EP5.

The above observation indicates that compared to EP20, there is obviously higher compatibility between the dispersed and matrix phases of EP5.

Therefore, the presence of residual *b*-copolymer in the insoluble fraction of EP5 sample indicates that there are higher interfacial adhesion and entanglements involved compared with the other samples. This may be the result of reduced size of dispersed phase particles and more uniform rubber particle distribution.

With increase in contact area between the two phases there are more likely greater entanglements and cocrystallization occurring in the interface of two phases where interfacial adhesion between the

dispersed phase and the matrix is intensified. This matches with the findings of Li et al.¹⁵

Thermal analysis

Figure 4 shows the second heating in DSC curves of EP5, EP10, and EP20 samples. As shown, the thermal behaviors of all samples are almost the same with very similar melting behaviors. Table II shows that ΔH is increased with the increase of switch frequency or with the decrease of the dispersed phase particle size. Also as shown in Figure 5, the same behavior may be observed in the cooling curves of the samples.

Generally, with the increase in switch frequency, no change is detected in the crystal structure of the alloys because T_m and T_C values are constant. In accordance with the reduction in the size of dispersed phase particles, the contact area of PP and EPR increases; consequently, ΔH of the samples increases

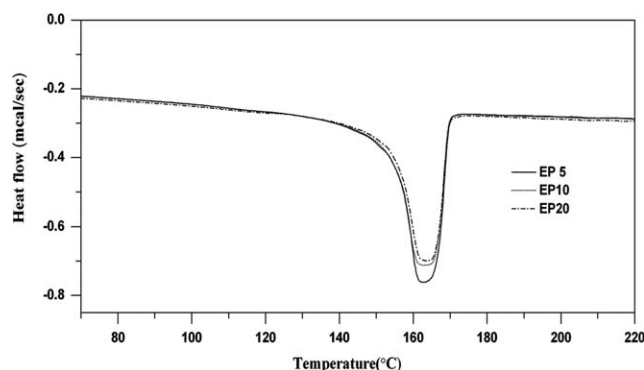


Figure 4 Melting DSC traces of PP/EPR in-reactor alloys.

because of slightly higher crystalline content in the interface as Chen et al. showed.⁸

Specifically in the case of EP5, with the increase in switch frequency, there are increases in its crystal content. These results are in agreement with the findings of Jiang et al.⁹ and Li et al.¹⁵ who showed that *b*-copolymer, being localized at the interface between the matrix and dispersed phases, functions as a compatibilizer. Because, as it is shown by ¹³C NMR data, *b*-copolymer is rich in PP and it does induce the cocrystallization of the surrounding dispersed phase. Therefore, it can be concluded that any increase in ΔH is related to the increase in crystal content of the contact area between the matrix and the dispersed phase particles. These results are strong confirmation of interfacial adhesion, as it is revealed in ¹³C NMR analysis sections.

Also the close melting points of all samples confirm that T_m and T_C are almost independent of switch frequency. This means that all crystals sizes of the alloys are the same in all samples with similar structures. These findings are consistent with GPC results which confirm identical structures for all samples.

Rheology

In our previous work, we studied rheological behavior at temperatures of 180, 210, 230, and 250°C of in-reactor alloy samples and found that 180°C is the optimum temperature for interfacial adhesion between the two dispersed and matrix phases. As, at higher temperatures phase separation occurs and

TABLE II
The DSC Results of PP/EPR In-Reactor Alloys

| Sample | T_m (°C) | ΔH (mcal g ⁻¹) |
|--------|------------|------------------------------------|
| EP5 | 162.6 | 22.3 |
| EP10 | 162.6 | 21.0 |
| EP20 | 163.0 | 19.3 |

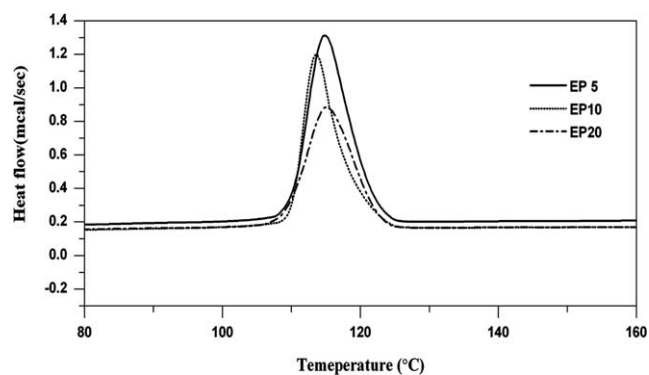


Figure 5 Cooling DSC traces of PP/EPR in-reactor alloys.

therefore, the rheological parameters of the alloy are not distinguishable.¹³ Figure 6 shows storage modulus (G') as a function of angular frequency (ω) for the samples EP5, EP10, and EP20 at 180°C. It can be seen that at low frequencies the storage modulus follows the sequence of EP5 > EP10 > EP20.

Scholz and Froelish¹⁶ and Graebing and Muller¹⁷ introduced some equations to model the rheological behavior of the blends and concluded that at low frequencies, the interface between the two phases plays a major role in the storage and loss moduli of the blend although the modulus of each phase is not accountable. At high frequencies, however, the modulus of each phase is high enough and therefore the modulus of the interface has no significant effect on the storage and loss moduli of the blend.

Obviously, storage modulus increases with the increase in switch frequency as a result of reduced particle size. This increase in the value of storage modulus is a result of greater interfacial area between the two phases.

Figure 7 provides the plot of η'' versus η' for the EP5, EP10 and EP20 samples. It is quite evident that there is partial compatibility between the two phases for all samples. Also it is shown, that there are significant differences between these samples in terms of viscosity. For EP5, the plot shows a bigger

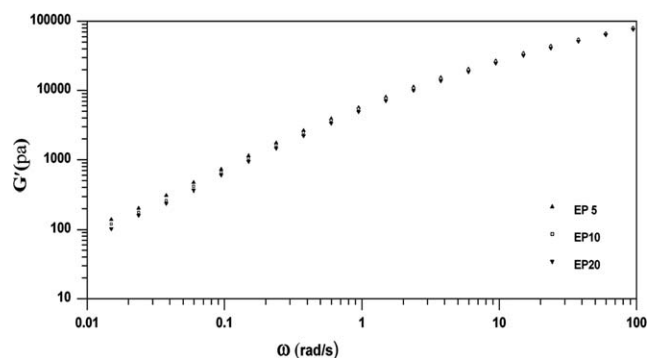


Figure 6 Storage modulus against angular frequency at 180°C.

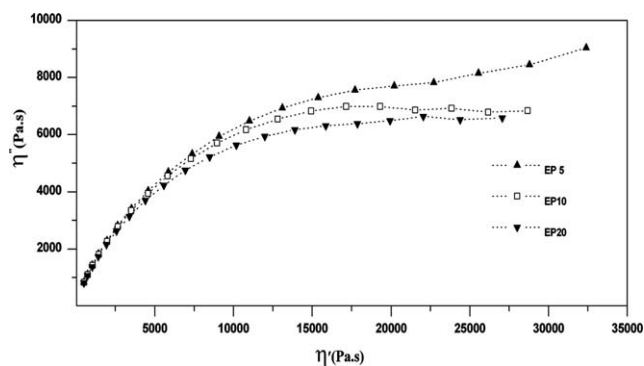


Figure 7 The η'' versus η' of PP/EPR in-reactor alloys at 180°C.

diameter compared to EP10 which is bigger than that for EP20. Cole-Cole plots are used to determine the miscibility or bimodality of amorphous or crystalline polymer blends and a good and smooth semi-circular shape suggests their good compatibility.¹⁸

This indicates that the interfacial adhesion in EP5 is higher than that of the other samples, confirming the better compatibility between the two dispersed and matrix phases.

It seems that with increase in switch frequency, particle size decreases and consequently the surface area of the dispersed phase particle increases. When dispersed phase is created in the copolymerization stage, each particle of dispersed phase is surrounded by some *b*-copolymers rich in PP produced acting as compatibilizing entities. Also, as particle size becomes smaller, the compatibility of the two phases increases, which is also in accordance with the findings reported by Xu et al.,⁷ Jiang et al.,⁹ and Li et al.¹⁵

The rheological results match the ¹³C NMR results shown in Figure 3. According to these results the higher interfacial adhesion between the two phases of EP5, revealed in the storage modulus and Cole-Cole graph, may be due to greater entanglements between the matrix and dispersed phase particles

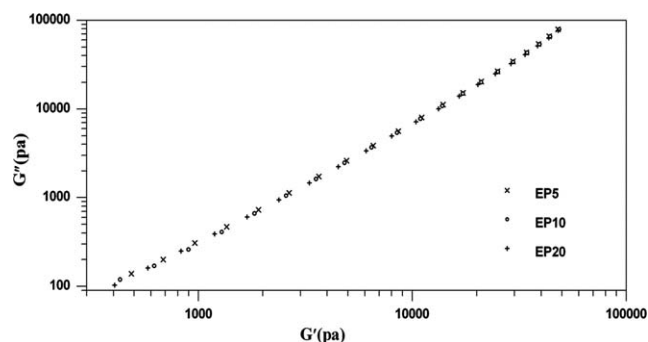


Figure 8 The plot of $G''-G'$ (Han plot) of PP/EPR in-reactor alloys at 180°C.

which are evident in ¹³C NMR spectra. This may also occur by higher cocrystallization at the contact area of the two phases as observed in the DSC curves of EP5.

The log-log profile of storage modulus (G') against loss modulus (G'') (Han plot), for different samples and at constant temperature (180°C), is presented in Figure 8. According to the rheological criterion established by Han et al.,^{19,20} the Han plot for a homogeneous and compatible blend is independent of temperature while giving a slope of 2 in its terminal region.^{21,22} They also found that such plots are independent of composition for compatible blends while being composition dependent for incompatible blends.

As shown in Figure 8, all samples show similar behavior, confirming the same composition existing in all. The slope is also an indication of good compatibility between the two phases. The same graph also shows the structural similarity of the blends. GPC results also confirm that the structure of the matrix and dispersed phases are unaffected by switch frequency.

Mechanical properties of the in-reactor alloys

Mechanical properties of the samples were measured and the obtained results are summarized in Figure 9(a,b). The impact strength of EP5 is much higher than that of EP20. The impact strength of the alloy has greatly improved by introducing higher

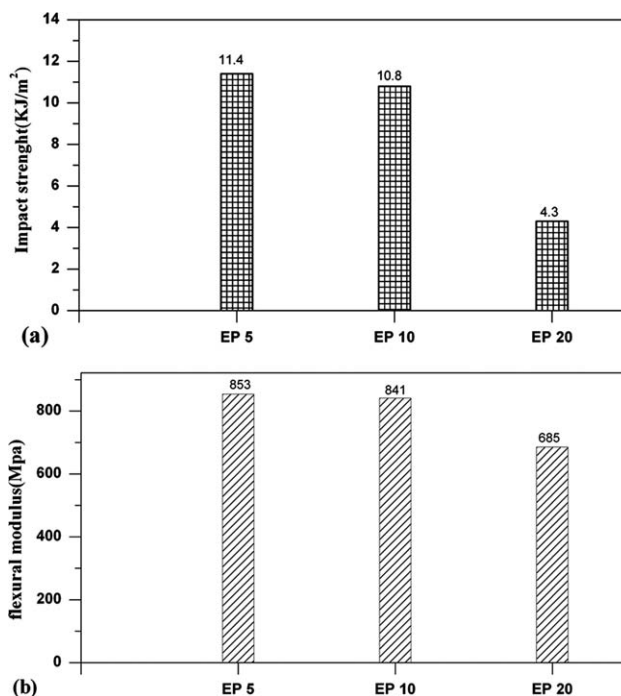


Figure 9 Mechanical properties of EP5, EP10 and EP20 (a) impact strength (b) flexural modulus.

switching frequency in the copolymerization stage, leading to increased compatibility or interfacial adhesion of the phases. Also the flexural modulus increased simultaneously with impact strength and matched the previous results obtained by Mei et al.¹¹ and Dong et al.¹² They showed that the materials produced by MZCR of Basell process show good balance between impact strength and rigidity.

This behavior is due to constant EPR content of all samples although the morphology and size of the dispersed phase are being different. Impact strength increases because of uniformity in distribution in the dispersed phase and increased flexural modulus is due to higher crystal content of EP5 sample where the greater role of matrix and crystalline interface between the matrix and the dispersed phase was shown by thermal analysis. Dong et al.¹² showed that with increase in switch frequency both impact strength and flexural modulus increased and concluded that increase in mechanical properties arises from greater uniformity in cavity distribution and also less EPR being pulled out due impact-fractured surface. Our results given in ¹³C NMR analysis confirm greater interfacial adhesion between the matrix and dispersed phases for EP5. Also these results match the data presented by rheological analysis, indicating that interfacial adhesion increases with increase in switch frequency and therefore the storage modulus and loss modulus increase together. These behaviors have not been explored in PP/EPR blends prepared by mechanical blending conducted by other researchers.^{23–25}

CONCLUSIONS

The molecular weight, its distribution and morphology of an in-reactor alloy of polypropylene (PP)/ethylene-propylene rubber (EPR), synthesized by multi-stage sequential polymerization, were investigated in relation to the thermal and mechanical properties and the rheological behavior of the alloy system.

The results indicate that altering switch frequency has no effect on the microstructure and molecular weight distribution of the polypropylene with very low effect on the synthesized EPR phase.

However, the morphological studies combined with rheological and mechanical investigations showed that increasing the switch frequency, reduced the size of the dispersed EPR leading to increase in mechanical performance due to increased interfacial adhesion and partial enhancement of crystalline content.

References

1. Maier, C.; Calafut, T. *Polypropylene*; Plastics Design Library a division of William Andrew Inc.: New York, 1998.
2. Pires, M.; Mauler, R. S.; Liberman, S. A. *J Appl Polym Sci* 2004, 92, 2155.
3. Kittilsen, P.; McKenna, T. F. *J Appl Polym Sci* 2001, 82, 1047.
4. Zhang, Y. Q.; Fan, Z. Q.; Feng, L. X. *J Appl Polym Sci* 2002, 84, 445.
5. Fan, Z. Q.; Zhang, Y. Q.; Xu, J. T.; Wang, H. T.; Feng, L. X. *Polymer* 2001, 42, 5559.
6. Lin, Z.; Peng, M.; Zheng, Q. *J Appl Polym Sci* 2004, 93, 877.
7. Xu, J. T.; Fu, Z. S.; Wang, X. P.; Geng, J. S.; Fan, Z. Q. *J Appl Polym Sci* 2005, 98, 632.
8. Chen, Y.; Chen, W.; Yang, D. *J Appl Polym Sci* 2008, 108, 2379.
9. Jiang, T.; Chen, H.; Ning, Y.; Kuang, D.; Qu, G. *J Appl Polym Sci* 2006, 101, 1386.
10. Xu, J. T.; Jin, W.; Fu, Z. S.; Fan, Z. Q. *J Appl Polym Sci* 2005, 98, 243.
11. Mei, G.; Herben, P.; Cagnani, C.; Mazzucco, A. *Macromol Symp* 2006, 51395, 677.
12. Dong, Q.; Wang, X.; Fu, Z. S.; Xu, J. T.; Fan, Z. Q. *Polymer* 2007, 48, 5905.
13. Bagheri, H.; Jahani, Y.; Nekoomanesh, M.; Hakim, S.; Fan, Z. Q. *J Appl Polym Sci*, Accepted.
14. Randall, J. C.; Hsieh, E. T. *Macromolecules* 1982, 15, 1584.
15. Li, Y.; Xu, J. T.; Dong, Q.; Fu, Z. S.; Fan, Z. Q. *Polymer* 2009, 50, 5134.
16. Scholz, P.; Froelish, D. *J Rheol* 1989, 33, 481.
17. Graebing, D.; Muller, R. *Colloid Surf* 1991, 55, 89.
18. Cho, K.; Ahn, T. K.; Lee, B. H.; Choe, S. *J Appl Polym Sci* 1997, 63, 1265.
19. Han, C. D.; Chuang, H. K. *J Appl Polym Sci* 1985, 30, 4431.
20. Han, C. D. *J Appl Polym Sci* 1986, 32, 3809.
21. Han, C. D.; Yang, H. H. *J Appl Polym Sci* 1987, 33, 1199.
22. Shucaï, L.; Pentti, K. J.; Pirkko, A. J. *J Appl Polym Sci* 1999, 71, 1649.
23. Kim, G. M.; Michler, G. H.; Gahleitner, M.; Fiebig, J. *J Appl Polym Sci* 1995, 60, 1391.
24. Karger, J.; Mouzakis, D. E. *Polym Eng Sci* 1999, 39, 1365.
25. Purnima, D.; Maiti, S. N.; Gupta, A. K. *J Appl Polym Sci* 2006, 102, 5528.